Near-surface Bipartition model for the study of material response of plasma-facing surfaces exposed to energetic charged particles

Deng Bai-Quan,[1,*] J. P. Allain,[2,**] Luo Zheng-Ming,[3]

Peng Li-Lin,[1] Yan Jian-Cheng[1]

[1] Southwestern Institute of Physics, P.O. Box 432, Chengdu 610041, China

[2] Argonne National Laboratory, 9700 South Cass Avenue, Argonne, IL 60439, USA

[3] Center of Radiation Physics, Sichuan University, Chengdu 610064, China

In order to predict the erosion rates and lifetimes of candidate plasma facing component (PFC) materials, the sputtering yields of Mo, W and deuterium-saturated Li surfaces bombarded by energetic charged particles were calculated by a new near-surface analytical sputtering model based on a bipartition model of charge particle transport theory. Lithium was considered as an alternative material providing low-recycling regime operation in advanced tokamak devices; expected charged-particle energies range from 100–1000 eV. Comparisons were made with Monte Carlo calculations of the TRIM code and experimental results, where available. The maximum sputtering yield of W by 3 keV He^+ ions, for example, was 0.032 and for Li by 0.4 keV He^+ ions was 0.17. Also calculated were the dependencies of maximum energy deposition and particle and energy reflection coefficients on the incident energy of energetic runaway electrons impinging on different material surfaces. The results are particularly important for estimating the lifetime of PFCs and analyzing the extent of impurity contamination, especially for high-power density and with a high plasma current fusion reactor.

Keywords: sputtering, bipartition model, transport theory, runaway electron

---

[*]Project supported by NNSF of China under Grant No 19889502, **Supported in part by DOE Contract No. DE-AC02-06CH11357.

Corresponding authors: both Deng Baiquan, Tel: 86 28 82932766, and Jean Paul Allain, Tel. 630 252 5184

E-mail: send to both dengbq@swip.ac.cn and allain@anl.gov

Mailing address: Deng Baiquan, Sichuan, Chengdu, P.O. Box 432, 610041; Fax: +86 28 82932 202

Introduction

The damaging effects of energetic charge particles on material surfaces in plasma-surface interaction research in fusion devices is one of the most important issues in determining fusion plasma performance and lifetime of plasma-facing components (PFCs) in fusion reactors [1]. For a high-power density fusion reactor with high plasma current during major disruption events, almost about 100 MW/m^2~1000 MW/m^2 average energy flux will be dumped on the PFC surface. The divertor target plate surface will endure much higher peak particle energy flux. Generally speaking, the damaging impact of energetic charge particles on material surfaces relates to several different fundamental processes, such as physical sputtering of material surface bombarded by energetic ions and electrons (i.e., electron-phonon coupling and vaporization), reflection of ions and electrons from the surface, secondary electron emission from the wall surface induced by incident ion and electrons, and ion implantation and re-emission. Among these processes, physical sputtering may be one of the most important in determining the erosion rate of the divertor plate and the extent of impurity contamination of the fusion core plasma [2]. The impurity concentration makes a decisive impact on the particle and energy balances of fusion plasma. The higher the impurity level, the less the fusion power produced because of fuel dilution and impurity radiation. Therefore, for an economically competitive fusion reactor, the impurity level must be kept as low as possible. Here we ignore erosion and redeposition effects as would exist in a real tokamak device. Rather, the focus is

on the damage incurred by materials facing the plasma whereby a sheath accelerates ions to the material surface at a particular incident angle. Incident angles studied here are normal with respect to the material surface, in order to guide comparisons to existing experimental data.

We have developed a new bipartition model of charged particle transport theory to calculate the sputtering yields of several candidate divertor materials [3, 4]. The physical sputtering process in fusion devices is due to energetic ions or atoms that escape from the scrape of layer and impinge on the material surface, undergoing a series of elastic collisions and depositing a fraction of their kinetic energies to atoms in the PFC surface. Recoiling atoms are produced in the damaged zone region, and those with sufficient energy generate secondary collisions, giving rise to next generation recoil atoms and leading to the development of a cascade. As a result, both the incident particles and the energetic recoil atoms can be scattered backward to the surface. If their kinetic energies are high enough to overcome the surface potential barrier, they can leave the surface and influx to the fusion plasma. This is the so-called sputtering process.

The sputtering phenomenon was discovered early last century but was not formulated theoretically until 1969, when Thompson and Sigmund [5] proposed the sputtering model based on the binary collision cascade concept. The semi-empirical formula for the sputtering yield calculation derived from their model predicted experimental results fairly well. However, the transport model still needed improvement. Their model included a backward transport equation, which was not a realistic description of cascade atoms going through the surface potential barrier and emitting into vacuum from the surface of the target material. Indeed, this equation is valid only for a homogeneous medium, whereas the medium at the surface is

nonhomogeneous and hence should be treated for the case of atoms being emitted from the surface.

To address this problem, we have developed a new quantitative physical sputtering theory based on a bipartition model of ion transport theory. This new model retains Sigmund's sputtering model, but the method describing cascade atoms is modified. In brief, the usual ion transport equation is directly used to describe the cascade collisions induced by the incident ion. In particular, the model includes a detailed description of the process of cascade atoms passing through the surface potential barrier leading to emission. Therefore, the formulation of a sputtering atom is described in more detail. From the viewpoint of the underlying physical mechanism, this method is similar to the application of Monte Carlo binary collision approximation simulation for study of the sputtering process. Both this new model and the Monte Carlo method retain Sigmund's three-step-model of the sputtering process, but the methods used to describe the atom cascade collisions are different. The former solves the transport equation of cascade atoms by using analytical transport theory, whereas the latter uses a statistical random sample method. Both methods should give very close sputtering yields if the same input parameters are used.

The main ideas of Sigmund's three-step-model are as follows. First, an impinging ion undergoes a series of elastic collisions in the target medium, and continuously deposits its energy to the target atoms. Second, the target atom acquiring sufficient energy breaks from the lattice and becomes a recoiling atom, which can move through the lattice. A recoiling atom with sufficient energy continues in turn undergoing secondary elastic collisions, giving rise to another generation of recoiling atoms and leading to the formulation of cascade atoms. Third,

a fraction of the cascade atoms move to the nearby material surface, and if their kinetic energy in the normal direction of the surface is greater than the surface potential barrier, then these atoms are emitted as sputtered atoms.

According to experimental studies of sputtering phenomena, the sputtering process usually happens within only 10~20-atom layers near the surface. One can therefore devise a simple model where the sputter yield is dependent only on the distribution function of incident ions near the surface and is independent of incident ion transport deep in the target material. In this study, we develop this new model as a complementary description of current sputter yield models. The sputtering yields for energetic H^+, D^+, T^+, and He^+ ion bombardment of three candidate PFC materials (Mo, W, and deuterium-saturated Li) are calculated and benchmarked both to experimental data and to Monte Carlo binary collision approximation simulation codes.

New sputter yield bipartition theoretical model

Sputtering takes place within only 10~20-atom layers close to the surface of the material (vacuum/material interface). This is the so-called emission thickness, or sputter depth. Under most circumstances, the energies of incident ions in a fusion device at the plasma edge are greater than 100 eV. Therefore, the implantation ranges of incident ions in the target medium usually are more than 100 Å. However, the thickness of 10~20-atom layer is about 10 Å. The distribution function of incident ions changes exiguously within the emission thickness and is quite close to the distribution function of incident ions at the surface. Therefore, it is reasonable to substitute the distribution function of incident ions at the surface for the

distribution function within the emission thickness. The distribution function at the surface $f_0^{(i)}(0,\mu,E)$ consists of two parts: the distribution function of primary incident ions at the surface, and the distribution function of reflected ions at the surface. The ion distribution function at the surface can be written as

$$f_0^{(i)}(0,\mu,E) \approx \delta(E-E_0)\delta(1-\mu)/2\pi + N(0,\mu,E)\,. \qquad (1)$$

The first term of Eq. (1) is the distribution function of directional incident ions with monoenergy, and the second term is the distribution function of the reflected ions at the surface.

The number of first-generation cascade atoms with energy $E \pm dE$ per unit volume and per unit energy interval generated by elastic collisions between the target atom and the primary incident ion or reflected ion can be given by

$$\begin{aligned} S^{(ia)} = N \int_{(E+E_d)/\gamma}^{E_0} dE' \int_{4\pi} d\vec{u}' f^{(i)}(0,\mu',E')\sigma_n^{ia}(E',E+E_d) \\ \times \delta(\vec{u}.\vec{u}' - \frac{M_1+M_2}{2M_1}\sqrt{\frac{M_1(E+E_d)}{M_2E'}})/2\pi, \end{aligned} \qquad (2)$$

and the intensity of the newly generated cascade atoms from elastic collisions between target atoms and cascade atoms knocked off from the lattice is

$$\begin{aligned} S^{(aa)} = N \int_{E+E_d}^{\gamma E_0 - E_d} dE' \int_{4\pi} d\vec{u}' f^{(a)}(x,\mu',E')\sigma_n^{aa}(E',E+E_d) \\ \times \delta(\vec{u}\cdot\vec{u}' - \sqrt{\frac{E+E_d}{E'}})/2\pi, \end{aligned} \qquad (3)$$

where N is the target atom number per unit volume; σ_n^{ia} is the differential cross section of elastic collisions between incident ions and target atoms, σ_n^{aa} is the differential cross section of elastic collisions between target atoms and cascade atoms, E_d is the average displacement

energy of target atoms and $\gamma = 4M_1M_2/(M_1+M_2)^2$ is the maximum energy transfer factor, M_1, E_0 are the mass and initial energy of the incident ions, M_2 is the mass of the target atoms, $\vec{u}$ and $\vec{u}'$ are the solid angles, and μ is the directional cosine of $\vec{u}$.

Based on the statistical balance principle, the distribution function of cascade atoms obeys the following transport equation:

$$\begin{aligned} &-\frac{\partial \rho_e^{(a)}(E) f^{(a)}(x,\mu,E)}{\partial E} + \mu \frac{\partial f^{(a)}(x,\mu,E)}{\partial x} = N \int_E^{\gamma E_0 - E_d} dE' \int_{4\pi} d\vec{u}' f^{(a)}(x,\mu',E') \\ &\times \sigma_n^{aa}(E', E'-E)\delta(\vec{u}\cdot\vec{u}' - \sqrt{\frac{E}{E'}})/2\pi - N f^{(a)}(x,\mu,E)\int_0^E d\tau \sigma_n^{aa}(E,\tau) \\ &+ S^{(ia)}(x,\mu,E) + S^{(aa)}(x,\mu,E), \end{aligned} \tag{4}$$

where $\rho_e^{(a)}(E)$ is the electronic stopping power of cascade atoms. Because cascade atoms undergo many types of collisions, the angular distribution of cascade atoms approaches a relatively isotropic distribution; hence the P_n -approximation is applicable. Then we have

$$f^{(a)}(x,\mu,E) \approx \sum_{l=0}^{n} \frac{2l+1}{4\pi} P_l(\mu) N_l^{(a)}(x,E). \tag{5}$$

Similarly, the P_n -approximation also can be made for $S^{(ia)}(x,\mu,E)$ and $S^{(aa)}(x,\mu,E)$ as follows.

$$\begin{aligned} S^{(ia)}(x,\mu,E) &\approx \sum_{l=0}^{n} \frac{2l+1}{4\pi} P_l(\mu) S_l^{(ia)}(x,E) \\ S^{(aa)}(x,\mu,E) &\approx \sum_{l=0}^{n} \frac{2l+1}{4\pi} P_l(\mu) S_l^{(aa)}(x,E) \end{aligned} \tag{6}$$

In Eq. (5), $N_l^{(a)}$ is the *lth* spherical harmonic moment of $f^{(a)}(x,\mu,E)$ and satisfies the following equation:

$$-\frac{\partial \rho_e^{(a)}(E) N_l^{(a)}}{\partial E}+\frac{1}{2l+1}\left[(l+1)\frac{\partial N_{l+1}^{(a)}(x,E)}{\partial x}+l\frac{\partial N_{l-1}^{(a)}(x,E)}{\partial x}\right]= \tag{7}$$
$$-\varphi_l^{(a)}(E)N_l^{(a)}(x,E)+S_l^{(ia)}(0,E)+S_l^{(aa)}(x,E), \qquad l\le n$$

where $S_l^{(ia)}(0,E)$ and $S_l^{(aa)}(x,E)$ are the *lth* spherical harmonic moments of the source terms in the P_n-approximation of $S^{(ia)}(x,\mu,E)$ and $S^{(aa)}(x,\mu,E)$ given by

$$S_l^{(ia)}(0,E)=\frac{N}{\mu_0}\sigma^{(ia)}(E_0,E+E_d)\times P_l\left(\frac{M_1+M_2}{2M_1}\sqrt{\frac{M_1(E+E_d)}{M_2E_0}}\right)P_l(\mu_0)$$
$$+N\int_{(E+E_d)/\gamma}^{E_0}dE'\sigma_n^{(ia)}(E',E+E_d)\times P_l\left(\frac{M_1+M_2}{2M_1}\sqrt{\frac{M_1(E+E_d)}{M_2E'}}\right)N_l^{(i)}(0,E') \tag{8}$$

$$S_l^{(aa)}(x,E)=N\int_{E+E_d}^{\gamma E_0-E_d}dE'N_l^{(a)}(x,E)\sigma_n^{(aa)}(E',E+E_d)\times P_l\left(\sqrt{\frac{E+E_d}{E'}}\right) \tag{9}$$

and $\varphi_l^{(a)}(E)$ is the scattering parameter for the cascade atom with energy E.

In order to calculate the sputtering yield, a boundary condition different from the Mark boundary condition (which is valid only for free surface case) is required to match Eq. (7). The effects of the surface barrier are taken into account in this boundary condition by introducing a critical angle ϑ_c, which is determined by the relation

$$\cos\vartheta_c=\mu_c=\sqrt{\frac{U}{E}}, \tag{10}$$

where U is the surface binding energy (or barrier potential). The proper boundary condition is

$$f^{(a)}(0,\mu_{i,}E)=\begin{cases} f^{(a)}(0,-\mu_i,E), & 0<\mu_i<-\mu_c \\ 0 & -\mu_c<\mu_i<1 \end{cases}, \tag{11}$$

where, $\mu_i(i=0,1,.....,n)$ are the roots of the Legendre polynomial $P_{n+1}(\mu)$. This boundary

condition refers to the following physical picture of cascade atoms in the vicinity of the surface. The cascade atoms in the angular interval of $\mu_c < \mu < 0$ are reflected back into the material bulk by the surface potential barrier, while only the atoms moving in the angular interval of $-1 < \mu < \mu_c$ emit from the surface. Having solved Eq. (7) with boundary condition Eq. (11), we can calculate the sputtering yield as follows.

$$Y = \int_0^{\gamma E_0} N_1^{(a)}(0, E)dE \qquad (12)$$

Deuterium-saturated surface

In most realistic conditions, the material PFC surface is saturated by fuel atoms of deuterium (or tritium) in a fusion device [6]. The PFC surface can be regarded as a multicomponent surface. In this case the expression derived by Sigmund [7] based on the linear cascade theory can be used to calculate the partial sputtering yield.

$$\frac{Y_{Li}}{Y} = \frac{c_{Li}}{c_D}\left(\frac{M_D}{M_{Li}}\right)^{2m}\left(\frac{U_D}{U_{Li}}\right)^{1-2m} \qquad (13)$$

To make comparisons with experimental data, we calculated here only the deuterium-saturated lithium. In Eq. (13) Y is the absolute sputtering yield, as given in Eq. (12), if no deuterium atoms are present on the lithium surface. C_D is the concentration of deuterium atoms in a lithium matrix, and $c_{Li} = 1 - c_D$. The U_{Li} and M_{Li} correspond to the surface binding energy and mass of lithium, which are equal to 1.67 eV and 6.97 amu, respectively. We assumed a 50%Li -50%D surface coverage and with a homogeneous composition profile. The assumption of deuterium dissolved in lithium with a 1:1 concentration is supported by recent experimental data of lithium surfaces exposed to tokamak plasmas and hydrogen isotope retention studies

by Mirnov et al. [8]. The surface binding energies are taken from Fig. 5 of Ref. [9]. The U_D must be replaced by the binding energy of the Li-D compound rather than pure solid phase deuterium; here we use 1.1 eV [10].

Results and Discussion

The sputtering yields of W and Mo bombarded at normal incidence by the energetic fusion charge particles H^+, D^+, T^+, and He^+ are calculated with the new sputter yield transport model. The results are shown in Fig. 1 and Fig. 2, respectively. For comparison, the Monte Carlo TRIM data [11] with D^+ and T^+ bombardment, as well as D on W experimental data [12], is plotted on the same figures. The sputter threshold for W sputtering is predicted to be high for light-particle bombardment. The bipartition model (BM) results compare reasonably well with experimental data of D bombardment of W. The threshold is about 300 eV for deuterium bombardment and about 700 eV for hydrogen bombardment. At energies higher than 1-keV both the BM and TRIM results are relatively close. Both BM and TRIM predict the sputter yield maximum to occur between and impact energy range of 2–4 keV for D bombardment and about 5 keV for H bombardment at normal incidence. The sputter threshold shifts to lower energies as the impact particle mass increases, and for tritium bombardment the threshold is low to about 200 eV. He bombardment yields the lowest sputter threshold near 200 eV. This result could be problematic for burning plasma machines such as ITER, where alpha physics could dominate and He could reach high concentration levels near 5% in the tokamak plasma. The bipartition model also predicts that W sputtering from bombardment by He ions can reach a maximum at lower particle energies compared to light-atom sputtering near 1-2 keV.

TRIM-SP simulations consistently predict a lower sputter threshold compared to the bipartition model. This difference in sputter threshold is more evident when comparing D and T bombardment on Mo surfaces. In this interaction, the bipartition model predicts a sputter threshold above 100 eV for D bombardment, whereas TRIM predicting this threshold to be below 100 eV. The sputter threshold for H bombardment on Mo is about 300 eV. Sputter maxima are also shown by the bipartition model to be different for Mo compared to W. Hydrogen bombardment of Mo reaches a sputter yield maximum near 2–3 keV and D bombardment between 1 and 2 keV. The maximum sputter yield of Mo is about a factor of 2 more than W when bombarded by He ions. As with W sputtering, the BM and TRIM results agree well for higher impact energies above 1 keV.

Figure 3 shows the sputtering yields of deuterium-saturated Li bombarded by He^+ and D^+ at normal incidence. Comparisons are shown with experimental data provided by Allain and Ruzic [13], the Sigmund sputter yield model based on transport theory, and Monte Carlo TRIM simulations for He on Li bombardment. The results obtained from the new model are in reasonable agreement with the Monte Carlo results from the TRIM code and Allain's experimental data. When assessing the complexity of the analytical tools employed, however, calculation by the new model is more effective at modeling the sputter threshold region compared to the Monte Carlo TRIM simulations. This data can be used to estimate the lifetime of plasma-facing components and to analyze the impurity level in core plasma of fusion reactors. D-saturated lithium has a much smaller sputter threshold compared to high-Z materials presented earlier. Lithium has a relatively low sublimation heat, and thus sputtering

thresholds are expected to be below 100 ev. The bipartition model predicts the sputter yield threshold to be between 0.04–0.05 keV for D bombardment and 0.03 eV for He bombardment. The sputter yield of Li is also very high compared to Mo and W at their maximum. The lithium sputter yield maximizes at about 0.1 Li/ion with energies ranging from 0.7 to 1.0 keV. Despite the higher sputter yields, lithium is attractive because of its low Z character and other properties such as low melting point (liquid surface) and high D-retention for low-recycling tokamak operation.

Another important aspect in the erosion of components (divertor, limiter, etc.) facing tokamak plasmas is the exposure to enhanced heat fluxes from transient or semi-transient events [14]. We have developed a new transport code, using the bipartition model for energetic electrons, to calculate the maximum energy deposition on different material surfaces for different energetic runaway electrons that escape from the core fusion plasma during a disruption event or plasma current collapse. These events lead to an increase in impinging heat flux on the wall. The results are shown in Fig. 4 and Fig. 5 for different wall materials. E_0 refers to the incident particle energy, $\left.\frac{dE}{dx}\right|_{max}$ is the maximum energy deposition on various candidate fusion reactor plasma-facing material surfaces for different runaway electron energies, and R_N and R_E are the particle reflection coefficient and energy reflection coefficient of energetic electrons, respectively. Since lithium has a potential application [15] as a liquid curtain for the first wall of the blanket in a high power density reactor, it is included in this analysis.

The results are compelling but not unexpected. In the case of graphite most of the energy

is absorbed in close magnitude to lithium for low impact energies. When the impact energy increases, the material dependence of the maximum energy deposition converges to values under 10 MeVcm^2/gram. Figure 5 shows that both Mo and W radiate large amounts of heat deposited compared to Li. These results make Li a good candidate to handle large heat flux deposition in tokamak transient and semi-transient events.

Conclusions

We have developed a new near-surface sputtering model for predicting the sputter threshold of candidate fusion device materials by analytical means. The model is an alternative approach to the classical transport theory of Sigmund. Our simple model analyzes the sputter yield by having it dependent only on the distribution function of incident ions near the surface and independent of incident ion transport deep in the target material. The approach is achieved by analyzing two parts: the distribution function of primary incident ions at the surface, and the the distribution function of reflected ions at the surface. Thus the ion distribution function at the surface includes contribution both from incident particles at the near surface region and from those particles reflected toward the surface.

Results show that the bipartition model is particularly effective in the sputter threshold regime where many-body effects near the surface can dominate. Our results also compare fairly well in this energy regime with known experimental data of D on W. Lithium sputter yields are also predicted with a high degree of accuracy and demonstrate that sputter thresholds can be an order of-magnitude lower for Li compared to W. Transient and semi-transient events in

tokamak plasmas lead to unusually large heat flux deposition to the plasma-facing component surfaces. This situation was simulated by using the bipartition model for runaway electrons. The results show that Li radiates a very small amount of energy deposited compared to other plasma-facing materials such as W and Mo.

References

[1] G. McCracken, P.E. Scott, Nucl. Fusion 19, 898 (1979) 901.

[2] J. Roth, Impurity Generation Processes in Particle-Surface Interaction: Data Status and Needs, in: R. Janev, H. Drawin (Eds.), Atomic and Plasma-Material Interaction Processes in Controlled Nuclear Fusion, Dordrecht, Elsevier, 1993, vol. 1.

[3] Z.M. Luo, S. Wang, Phys. Rev. B.36 (1987) 1885.

[4] Z.M. Luo, Q. Hou, J. Appl. Phys. 74 (1993) 6007.

[5] P. Sigmund, Phys. Rev. 184 (1969) 383.

[6] J.P. Allain and D.N. Ruzic, Deuterium Treatment Effects on Lithium and Tin-Lithium Sputtering in Solid and Liquid Phase, in: A. Hassanein (Ed.), NATO Science Series: Hydrogen and Helium Recycling at Plasma Facing Materials, Vol. 54, Kluwer Academic Publishers, Dordrecht, 2002, p. 73.

[7] P. Sigmund, Sputtering by Particle Bombardment I, in: R. Behrisch (Ed.), Topics in Applied Physics, Springer-Verlag, Berlin, 1981.

[8] S.V. Mirnov, E.A. Azizov, V.A. Evtikhin, V.B. Lazarev, I.E. Lyublinski, A.V. Vertkov, D. Yu. Prokhorov, Plasma Physics and Controlled Fusion 48 (2006) 821.

[9] J. Roth, Physics of Plasma-Wall Interactions in Controlled Fusion, Plenum Press, New

York, p. 351.

[10] J.P. Allain, M.D. Coventry, D.N. Ruzic, J. Nucl. Mater. 313-316 (2003) 645.

[11] J. Biersack, W. Eckstein, *Appl. Phy*s A34 (1984) 73.

[12] W. Eckstein, C. Garcia-Rosales, J. Roth, W. Ottenberger, Sputtering Data, IPP Report 9/82, 1993.

[13] J.P. Allain, D. Ruzic, *Nucl. Fusion* 42 (2002) 202.

[14] A. Hassanein, J.P. Allain, Z. Insepov, I. Konkashbaev, Fusion Science and Tech. 47 (2005) 686.

[15] B.Q. Deng, J.H. Huang, J.C. Yan, L.L. Peng, E.Y. Wang, J. Nuclear Materials 313-316 (2003) 630.

Figure Captions

Fig. 1. Sputtering yield of tungsten bombarded by fusion light particles: H, D, T, and He calculated by new bipartition model (BM) compared to the Monte Carlo BCA TRIM code.

Fig. 2. Sputtering yield of molybdenum bombarded by fusion light particles: H, D, T, and He calculated by new bipartition model (BM) compared to the Monte Carlo BCA TRIM code.

Fig. 3. Sputter yield results of D-saturated solid lithium bombarded by D and He using the bipartition model (BM) compared to experimental data by Allain and Ruzic [13] and the Sigmund sputter yield theory.

Fig. 4. Maximum energy deposition versus runaway electron energy for different candidate fusion device PFC materials.

Fig. 5. Particle and energy reflection coefficients of energetic electrons on various candidate fusion device materials.

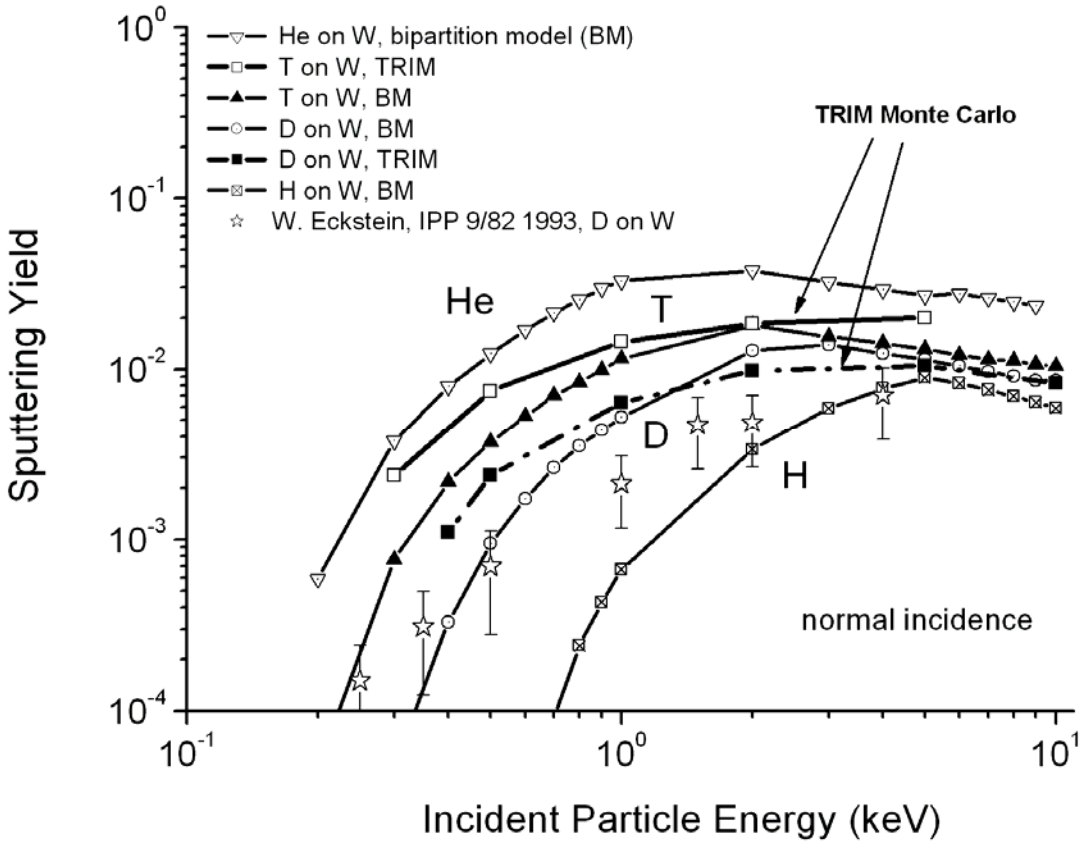
He on W, bipartition model (BM)
T on W, TRIM
T on W, BM
D on W, BM
D on W, TRIM
H on W, BM
W. Eckstein, IPP 9/82 1993, D on W
TRIM Monte Carlo
He
T
D
H
normal incidence
Sputtering Yield
Incident Particle Energy (keV)
10^0
10^-1
10^-2
10^-3
10^-4
10^-1
10^0
10^1

FIG. 1

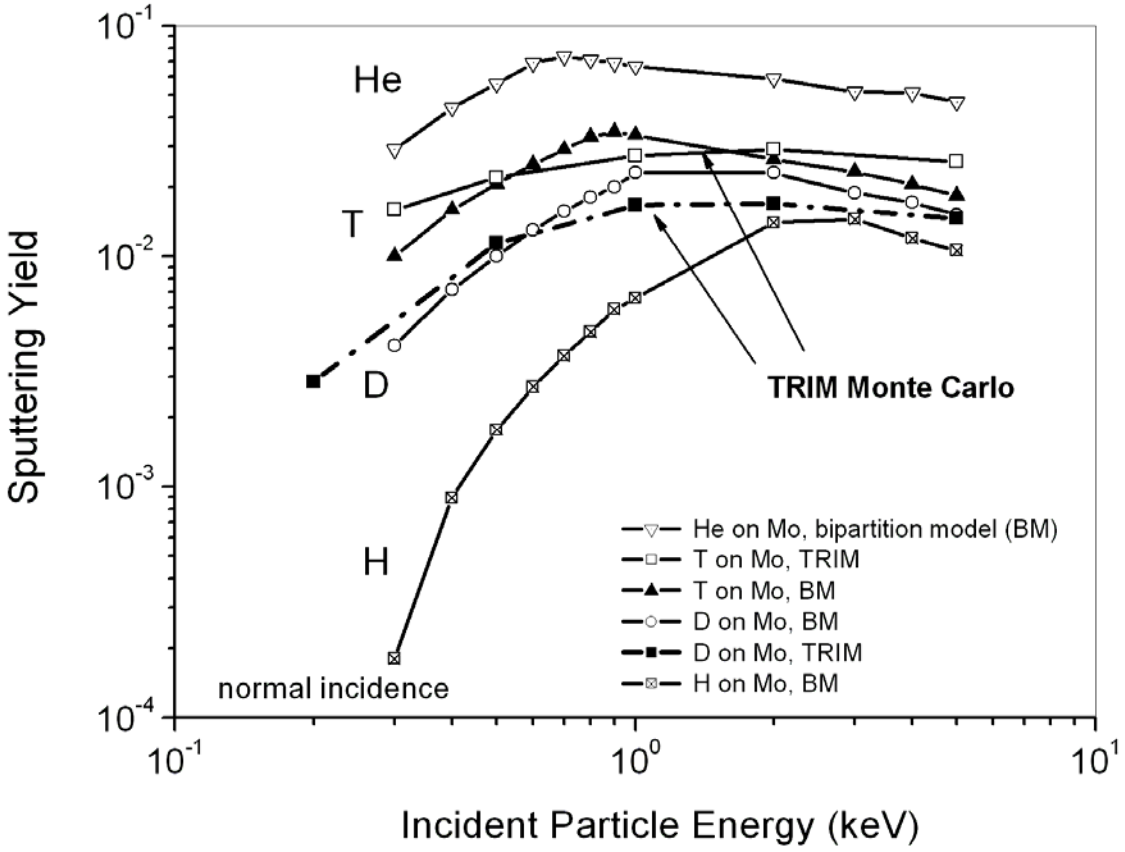
Sputtering Yield
Incident Particle Energy (keV)
He
T
D
H
TRIM Monte Carlo
normal incidence
He on Mo, bipartition model (BM)
T on Mo, TRIM
T on Mo, BM
D on Mo, BM
D on Mo, TRIM
H on Mo, BM

FIG. 2

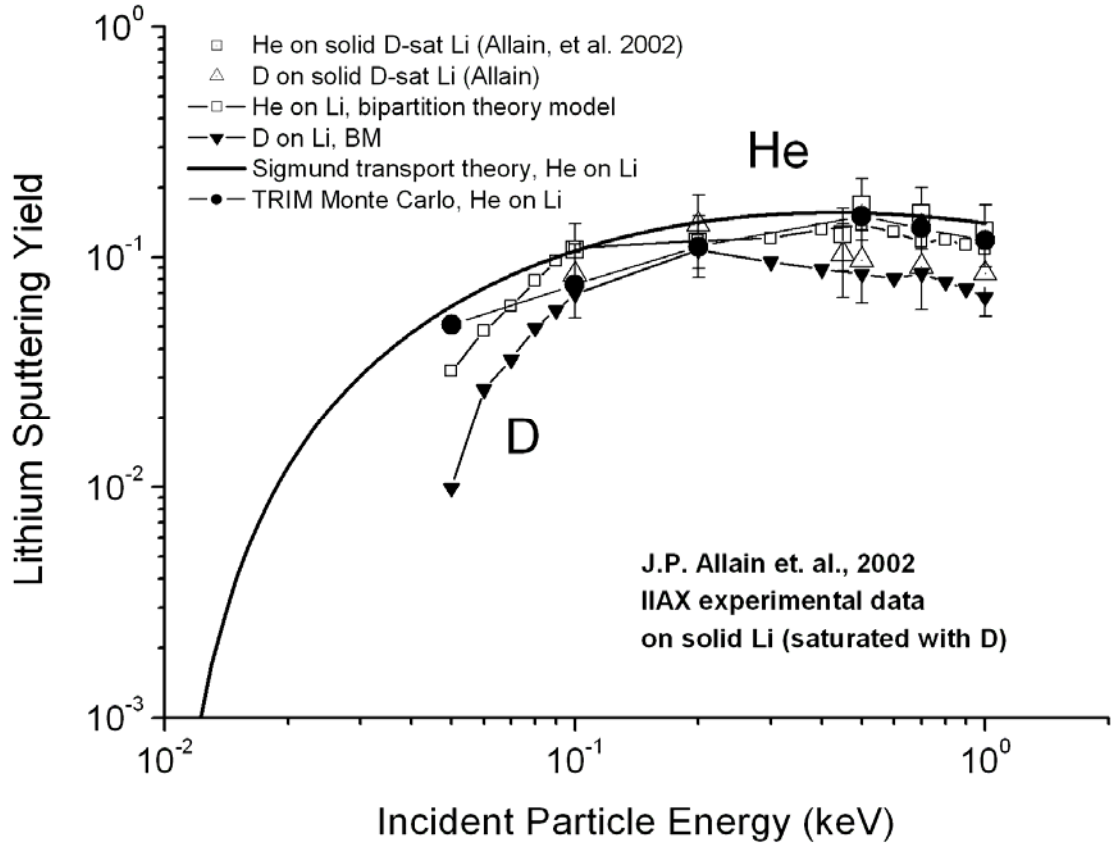
He on solid D-sat Li (Allain, et al. 2002)
D on solid D-sat Li (Allain)
He on Li, bipartition theory model
D on Li, BM
Sigmund transport theory, He on Li
TRIM Monte Carlo, He on Li
He
D
J.P. Allain et. al., 2002
IIAX experimental data
on solid Li (saturated with D)
Lithium Sputtering Yield
Incident Particle Energy (keV)
10^0
10^-1
10^-2
10^-3
10^-2
10^-1
10^0

FIG. 3

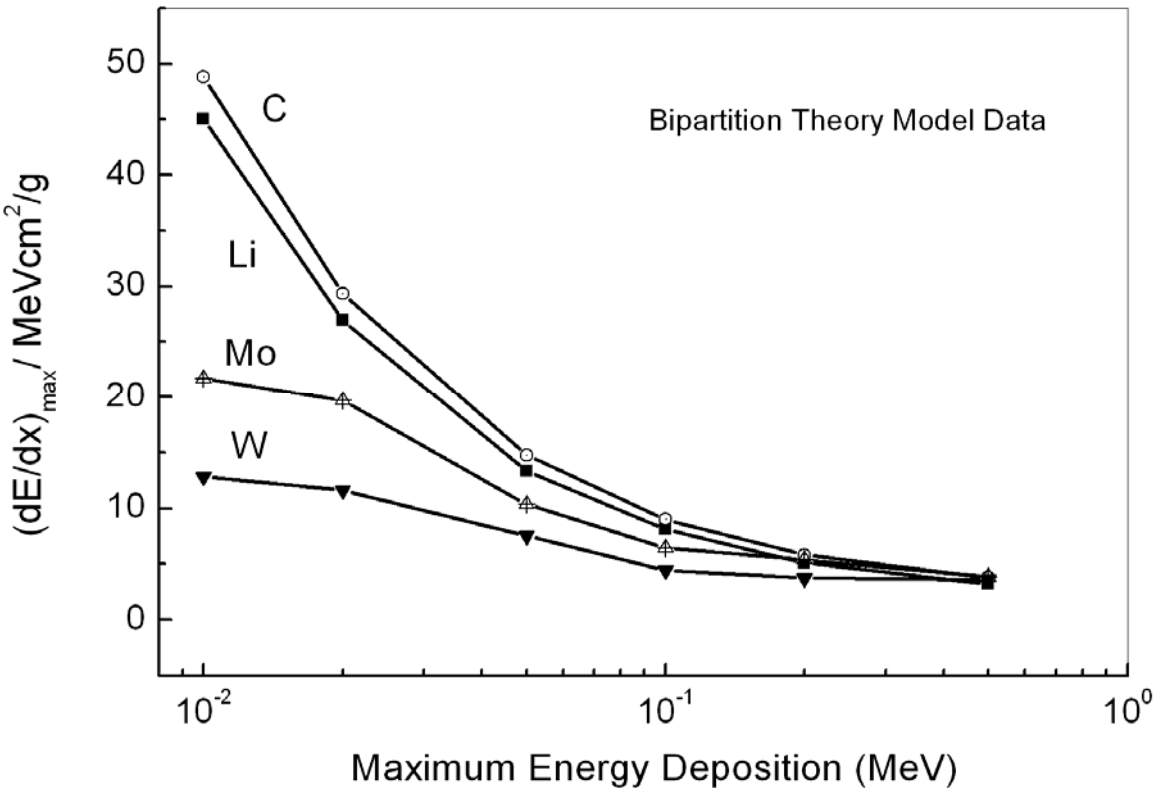
Bipartition Theory Model Data
C
Li
Mo
W
50
40
30
20
10
0
10^{-2}
10^{-1}
10^{0}
$(dE/dx)_{max}$ / MeVcm^2/g
Maximum Energy Deposition (MeV)

FIG. 4

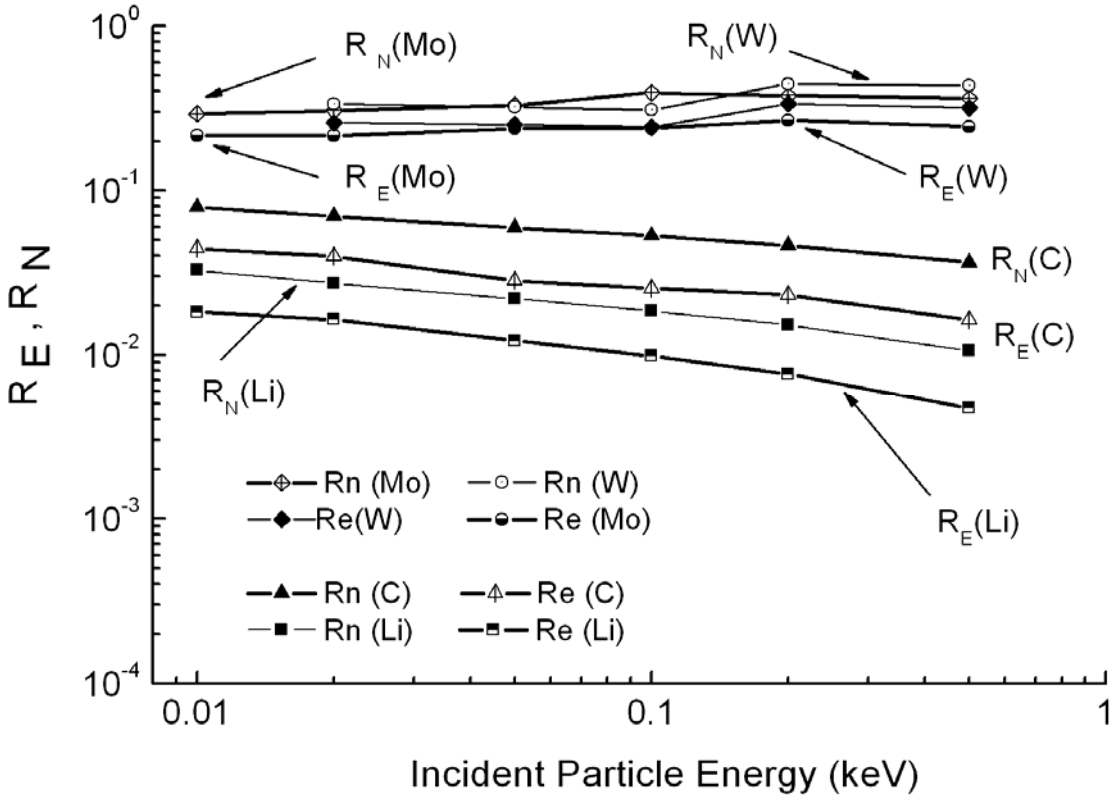
10^0
10^{-1}
10^{-2}
10^{-3}
10^{-4}
R E , R N
0.01
0.1
1
Incident Particle Energy (keV)
R N(Mo)
R N(W)
R E(Mo)
R E(W)
R N(C)
R E(C)
R N(Li)
R E(Li)
Rn (Mo)
Rn (W)
Re(W)
Re (Mo)
Rn (C)
Re (C)
Rn (Li)
Re (Li)

FIG. 5